


## Article

# Analysis of Supraharmonics Emission in Power Grids: A Case Study of Photovoltaic Inverters

João Pinto <sup>1</sup>, Bernhard Grasel <sup>2</sup>  and José Baptista <sup>1,3,\*</sup> 

<sup>1</sup> Department of Engineering, University of Trás-os-Montes and Alto Douro, 5000-801 Vila Real, Portugal; al71824@alunos.utad.pt

<sup>2</sup> Competence Field Renewable Energy Technologies, University of Applied Sciences Technikum Vienna, 1200 Vienna, Austria; grasel@technikum-wien.at

<sup>3</sup> INEC-TEC UTAD Pole, University of Trás-os-Montes and Alto Douro, 5000-801 Vila Real, Portugal

\* Correspondence: baptista@utad.pt

**Abstract:** High-frequency (HF) emissions, referred to as supraharmonics (SHs), are proliferating in low- and medium-voltage networks due to the increasing use of technologies that generate distortions in the 2 kHz to 150 kHz range. The propagation of SHs through the electrical grid causes interference with power supply components and end-user equipment. With the increasing frequency of these incidents, it is imperative to establish guidelines and regulations that facilitate diagnosis and limit the amount of emissions injected into the electrical grid. The proliferation of SH emissions from active power electronics devices is a significant concern, especially considering the growing importance of photovoltaic (PV) systems in the context of climate change. The aim of this paper is to address and analyze the emissions from different PV inverters present in an electrical network. Several scenarios were simulated to understanding and identifying possible correlations. This study examines real signals from PV systems, which exhibit narrowband, broadband and time-varying emissions. This paper concludes by emphasizing the need for specific regulations for this frequency range while also providing indications for future research.

**Keywords:** power quality; supraharmonics; photovoltaic generation system; power electronic converters; high-frequency emissions; intermodulation and propagation



**Citation:** Pinto, J.; Grasel, B.; Baptista, J. Analysis of Supraharmonics Emission in Power Grids: A Case Study of Photovoltaic Inverters. *Electronics* **2024**, *13*, 4880. <https://doi.org/10.3390/electronics13244880>

Academic Editor: Sonia Leva and Pablo García Triviño

Received: 10 October 2024

Revised: 1 December 2024

Accepted: 6 December 2024

Published: 11 December 2024



**Copyright:** © 2024 by the authors. Licensee MDPI, Basel, Switzerland. This article is an open access article distributed under the terms and conditions of the Creative Commons Attribution (CC BY) license (<https://creativecommons.org/licenses/by/4.0/>).

## 1. Introduction

As consumers become more aware of energy and environmental issues, an increase in the adoption of grid-connected PV panel installations is expected, promoting decentralized electricity generation.

The Paris Agreement, signed in 2015, represents a paradigm shift in society, with the explicit recognition that only through the contribution of all can the challenge of climate change be overcome. This voluntary agreement outlines that each country defines its own “Nationally Determined Contributions” (NDCs) to the global effort of reducing emissions [1]. Portugal, for instance, has committed to achieving Carbon Neutrality by 2050, having developed the Roadmap for Carbon Neutrality 2050 (RNC2050) [2], which establishes the trajectories and guidelines for the policies and measures to be implemented within this timeframe. Additionally, Instruction No. 3/2020, which transposes Directive (EU) 2019/944 [3] and Directive (EU) 2018/2001 [4] of the European Parliament and the Council, approves the draft contract for the acquisition of electricity by the last resort supplier from producers, also applying to surplus energy produced under self-consumption regimes. This regulation places particular emphasis on PV systems. This creates all the conditions for mass adoption.

The integration of PV systems into power grids has become increasingly prevalent, being driven by the growing demand for renewable energy sources. However, the integration of these systems can introduce various power quality issues, including the injection of

SHs into the grid. SHs, defined as frequency components above 2 kHz, can have significant impacts on the operation and stability of power grids [5].

This research paper aims to analyze the emission of SHs in power grids caused by the integration of PV inverters. The study considers the potential issues that can arise from the integration of PV systems, including harmonic distortion, voltage fluctuations, and voltage asymmetry [6,7]. There are now studies analyzing SH emissions from electric vehicle fast-charging stations [8]. The paper also explores the impact of various penetration levels of PV generation on the distribution network, with a focus on identifying the optimal placement of PV systems to mitigate potential power quality issues.

This study is based on the guidelines of other authors who have analyzed the impact of PV systems on power quality. One study found that while harmonic distortion and the voltage profile can improve with the integration of PV systems, voltage asymmetry can increase, although it remains within the allowed range due to the injection of DC components. Another study highlighted the potential for power electronics equipment to introduce electromagnetic disturbances and the need for effective technical solutions to mitigate these issues [9].

The secure interconnection of PV systems to the electrical grid requires strict compliance with standards such as the IEC 61000 series, IEEE-519 [10], or IEEE-1547 [11], thereby limiting the level of PV system penetration in the grid to ensure the stability and quality of the power supply.

Previously, the conversion of direct current (DC) to alternating current (AC) and vice versa was predominantly carried out using passive power electronics, with converters utilizing diodes or thyristors. This approach resulted in significant harmonic emissions in the frequency range up to 2 kHz. However, technological advancements have introduced materials such as silicon carbide (SiC) and gallium nitride (GaN) in power electronics switches, such as IGBT and MOSFET, allowing for a substantial increase in conversion efficiency. Although these technologies lead to lower harmonic distortion at frequencies up to 2 kHz, greater distortions are observed at higher frequencies (>2 kHz) due to the high switching frequencies involved [12]. The SH emissions resulting from switching frequencies are caused by PWM modulation, and these emissions are visible in the frequency spectrum and its multiples [13,14].

Currently, various methodologies are being employed for the measurement of SH emissions, including IEC61000-4-7 [15] and IEC61000-4-30 [16] standards. While the method outlined in IEC61000-4-7 is based on continuous measurement using 200 Hz frequency bands, IEC61000-4-30 specifies a non-continuous grouping method in which 2 kHz frequency bands are used. Another methodology is the CISPR-16 [17] standard, which is widely used for conducting electromagnetic interference measurements, covering disturbance and immunity testing. At present, SH emissions are not subject to specific regulatory limits, as shown in Figure 1. The measurement procedure according to IEC61000-4-30 is currently under consideration in IEC SC 77A WG9 and will be adapted due to the lack of signal coverage (only 8%) and the lack of real signal representation due to the 2 kHz band grouping method, where signal information is lost [18].

When analyzing, for example, the interaction of SH emissions between a PV inverter and an electric vehicle, there is a phenomenon that has been extensively researched in the literature, especially within telecommunications—known as intermodulation distortion—is observed [19]. Resulting from the interaction between the different switching frequencies of the devices involved, intermodulation distortion emerges as a critical issue. It introduces new frequency components into the grid, increasing the potential for interference with connected devices and necessitating rigorous analysis to ensure the stability and effective functionality of the energy system.

There needs to be a distinction between the standards relating to SHs. It is notoriously known that there are standards that limit the amount of emissions present in public grids. First, there are standards of already-implemented compatibility levels for SH emissions such as the IEC61000-2-2:2002 [20]. The EN50160 defines informative limit values. The

compatibility levels for harmonic distortion in low-voltage grids are currently under revision by the IEC SC77A WG8 [21]. And standards that limit emissions from a single equipment also exist.

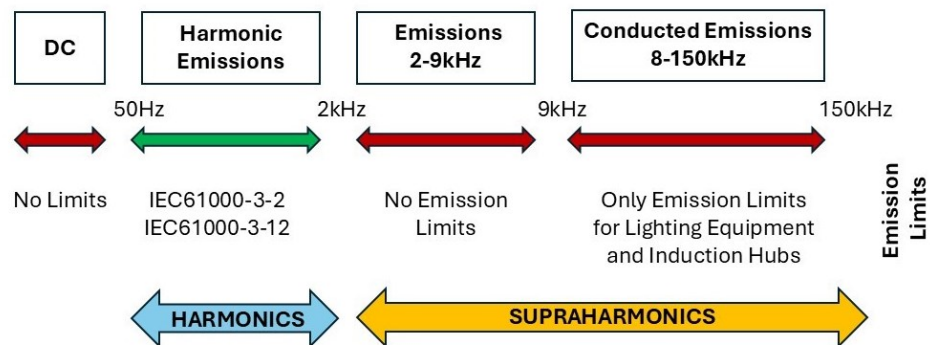


**Figure 1.** Emission range and compatibility with international standards.

The electrical signal is a versatile entity that can be analyzed and understood in both the time and frequency domains. This work aims to explore the interactions between these two domains, with the objective of studying the propagation of SH emissions from PV systems. Despite recent advancements, there remains a significant knowledge gap in understanding the formation mechanism and propagation characteristics of SH distortion.

The subsequent sections of the paper are organized as follows: Section 2 presents a simplified model for the SH emissions produced in PV systems, including an index for assessing power quality and a brief description of the existing standards for SH measurement. Section 3 describes the electrical grid under study, the methodology, and the equipment used. Section 4 presents the main results obtained, discussing the key points in accordance with the findings. Finally, Section 5 outlines the main conclusions of the paper and future work.

## 2. Supraharmonics

SHs denote electrical signals present in power systems at frequencies above the typical harmonic range, specifically between 2 kHz and 150 kHz. These are higher-frequency disturbances that can arise from modern power electronics, renewable energy sources, or other non-linear loads. The mathematical background for SHs involves several key areas, primarily rooted in signal processing, Fourier analysis, and power system theory. At the core of SHs analysis is the concept of Fourier analysis, which allows for the decomposition of any periodic signal into its sinusoidal components. Traditional harmonic analysis focuses on multiples of the fundamental frequency (e.g., 50 Hz or 60 Hz in power systems), but for SHs, the analysis extends to higher frequencies. For periodic signals, the Fourier series is used to express the signal as a sum of sines and cosines. Given a periodic function  $f(t)$  with period  $T$ , it can be expressed by Equation (1) [22].

$$f(t) = a_0 + \sum_{n=1}^{\infty} \left( a_n \cos \frac{2\pi n t}{T} + b_n \sin \frac{2\pi n t}{T} \right) \quad (1)$$

where  $a_0$  is the constant (DC) component, representing the average value of the function over one period. The terms  $a_n$  and  $b_n$  are the Fourier coefficients, representing the amplitudes of different frequency components.

Since supraharmonic signals are often analyzed digitally, the sampling theorem plays an important role. The Nyquist criterion states that to capture all frequency components of a signal without aliasing, the sampling frequency  $f_s$  must be at least twice the maximum frequency of interest  $f_{max}$ , which is given by Equation (2).

$$f_s \geq 2 \cdot f_{max} \quad (2)$$

For supraharmic analysis, where frequencies extend to 150 kHz, the minimum sampling rate should be higher than 300 kHz to ensure accurate signal representation.

When analyzing SH emissions, it is of utmost importance to make a clear distinction between primary and secondary emissions. When measuring the SH emissions of an electrical device at a Point of Common Coupling (PCC), one is always measuring the sum of both primary and secondary emissions [23]. This differentiation is crucial for identifying the source of the emissions, whether from the device under test or from external sources, which is essential for correctly assigning responsibility. However, this process faces considerable complexity, as it is often not feasible to isolate a single device to determine its primary emissions, whether in laboratory conditions or in field measurements.

A simplified theoretical model to facilitate the understanding of primary and secondary emissions is to represent SH emissions from a device, such as a photovoltaic system, as a constant source of supraharmic current accompanied by an internal impedance, which serves to absorb a portion of the emissions. In this context, the primary emission is partially distributed through the electrical grid, while an additional fraction passes through the impedance associated with another device connected nearby. Thus, the total emission of the second device will consist of both its primary emissions and the secondary emissions derived from the first device. Background emissions from the grid can be appropriately represented by a voltage source, which creates a current through the impedance [24]. In practice, there is often a lack of clarity regarding how these impedances interrelate, complicating the distinction between primary and secondary emissions. Additionally, it becomes challenging to determine a device's primary emissions when it is not connected to an undisturbed network.

### 2.1. Effects of SH Emissions

SH emissions have emerged as a significant power quality concern due to the increasing use of power electronics in modern grids [25]. These emissions can cause various negative effects, including power loss, heating of the grid elements, aging of the dielectric materials, and interference with equipment and power line communication [26]. SHs can lead to malfunctions in control circuits, impact LED lamp intensity, and accelerate aging of the capacitors, transformers, and rotating machines [26]. The thermal stress on components, particularly aluminum electrolytic capacitors in lighting equipment, is a notable long-term effect [21]. To address these issues, researchers have focused on developing methods for identifying, measuring, and mitigating SH emissions, as well as establishing new standards [27]. However, further research is needed to improve mitigation strategies and measurement techniques for SHs.

The skin effect is one of the major concerns: it causes the current in good conductors to concentrate more on the surface as the frequency increases, reducing the effective area for conduction. This increases electrical resistance and leads to greater heating in the cables and components of the electrical system. In addition to the mentioned thermal increase in components, additional effects are observed, such as perceptible sound emissions (20 Hz to 20 kHz, which is the human auditory range) and the malfunctioning of equipment, including PLC communication systems [28]. In order to evaluate the entire SH emission, in analogy to the total harmonic current, the  $TSHC_w$  is defined [28] by Equation (3):

$$TSHC_w = \sqrt{\sum_{bin,n}^n SH_{bin,n}^2 \cdot w_n} \quad (3)$$

This evaluation employs a frequency domain approach, where  $SH_{bin,n}$  represents the amplitude of each frequency bin, grouping bands from 2 kHz to 150 kHz, and subsequently comparing these bands with risk areas, considering the most harmful frequencies and assigning corresponding weights to these areas, which are defined as  $W_n$ .

When analyzing the HF emission spectrum, we observe the presence of both broadband and narrowband emissions. Figure 2a represents a snapshot in the time domain for

one of the simulations conducted. Figure 2b shows the equivalent representation in the frequency domain.

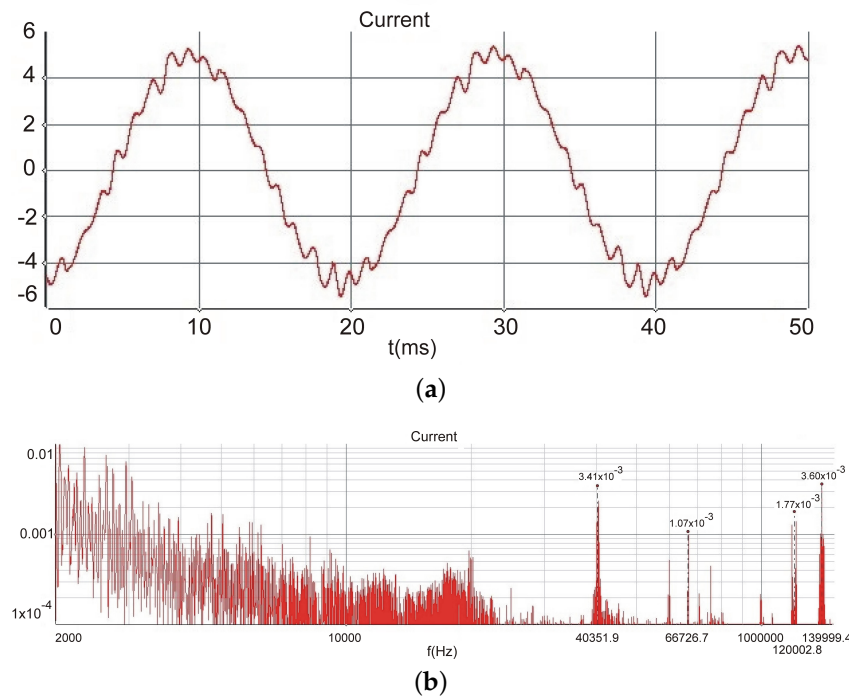


**Figure 2.** Measurement signals: (a) current time domain measurement; (b) SH spectrum (frequency domain measurement).

### 2.2. Measurement of SH Emissions

In the analysis of Figure 3, which illustrates the frequency spectrum of one of the measurements taken, the presence of emissions in the 2 kHz to 150 kHz range is observed. It is important to highlight that, in the context of SH emissions, isolated components are not observed, as are often identified with harmonics. Instead, these emissions typically manifest as a range or even as a set of components, whose width is not fixed and can vary considerably over time, making prior prediction difficult. As stipulated by the IEC standards, it is possible to segment frequencies into 2 kHz groups or even smaller 200 Hz groups. This approach results in components that are not confined to a single group but may extend across the boundaries of two groups. Thus, standardizing emission limits and structuring the spectrum into groups, rather than focusing on the analysis of isolated components, would be beneficial, as the latter proves to be a complex task [18].

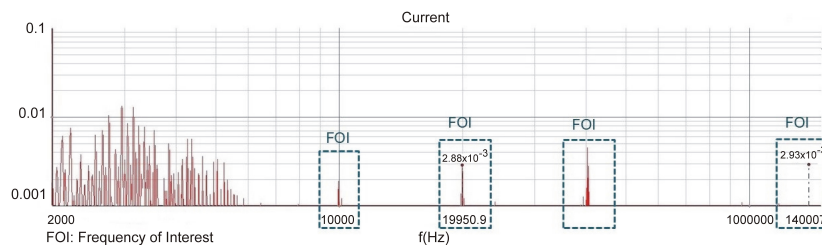


**Figure 3.** Representation of SH emission bands in an electrical system.

When analyzing SH emissions, it is essential to make a clear distinction between primary and secondary emissions. This distinction is crucial in order to identify the source of the emissions, whether they originate from the equipment under testing or from external sources, which is essential for the proper attribution of responsibilities. A simplified

theoretical model has been proposed to help understand primary and secondary emissions, as shown in Figure 4.

In this representative diagram, equipment 1 is represented as a constant source of SH current, denoted as  $I_{s1}$ , accompanied by an internal impedance,  $Z_1$ , which acts to absorb part of the emissions. This configuration gives the primary emissions of equipment 1, denoted as  $I_1$ , as described in Equation (4):

$$I_1 = I_{s1} \frac{Z_1}{Z_{grid} + Z_2 + Z_1} \quad (4)$$

where  $Z_1$  and  $Z_2$  are the internal impedances of equipment 1 and 2, respectively, and  $Z_{grid}$  is the network impedance; the primary emission ( $I_1$ ) is partially distributed through the electrical network, while an additional fraction flows through the impedance associated with equipment 2, as described in Equation (5):

$$I_{1,2} = I_1 \frac{Z_{grid}}{Z_{grid} + Z_2} \quad (5)$$

where ( $I_{1,2}$ ) is the emission from equipment 2 originating from equipment 1. Following the procedure described in Equation (4), it is possible to determine the primary emissions of equipment 2. However, the total emission from equipment 2 will be the integration of its primary emission ( $I_2$ ) and the secondary emission from equipment 1.

The total emissions from equipment 1 include a fraction of the emissions from equipment 2 that pass through its internal impedance  $Z_1$ . In addition, it becomes difficult to determine the primary emissions of a device when it is not connected to an undisturbed network, and it is often impractical to isolate a single device to determine its primary emissions, as was observed during the measurements.

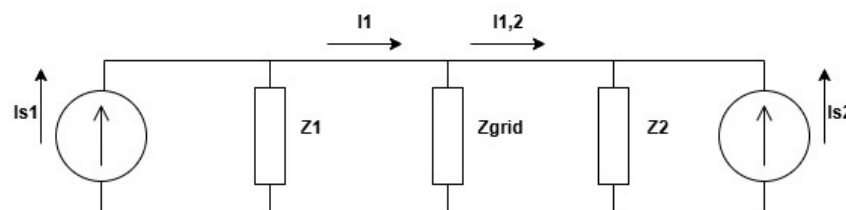


**Figure 4.** Simplified model for the characterization of the primary and secondary emissions of a piece of equipment.

### 3. Methods

This section describes the methodology employed in this paper, being aimed at exploring the impacts of SH emissions from PV inverters on an electrical distribution network. The approach chosen for this study is a combination of quantitative and qualitative methods, allowing for a detailed analysis that provides an objective view of the variables of interest. The justification for selecting this approach lies in the need to quantify interactions and measure the intensity of SH emissions resulting from PV systems. The qualitative approach, on the other hand, seeks to understand concepts and behaviors, with the aim of gaining a deeper understanding of the behavior of PV inverters.

The research was guided by thoroughly detailed scenarios that enabled the exploration of various situations relevant to the topic, aiming to shed light on the complexities inherent to this phenomenon. The primary question that directed this investigation asked the following: "Is it possible to quantify and understand the characteristics of SH emissions from PV systems?".

### 3.1. Smart Grid Lab at University of Applied Sciences Technikum Wien

At UASTW, the first laboratory featuring a Smart Grid from Austria was established. Given the crucial importance of the distribution network in integrating renewable energy sources, a distribution network was meticulously replicated.

This laboratory is connected to the public grid through a 630 kVA transformer and has an additional transformer for voltage control. The typical impedance of a distribution network is replicated using inductances and resistances. Different network topologies, such as ring or radial connections, can be implemented. Up to four branches with prosumer households, equipped with PV systems, storage, and electric vehicle charging, can be connected. Figure 5 illustrates the single-line diagram of the laboratory.

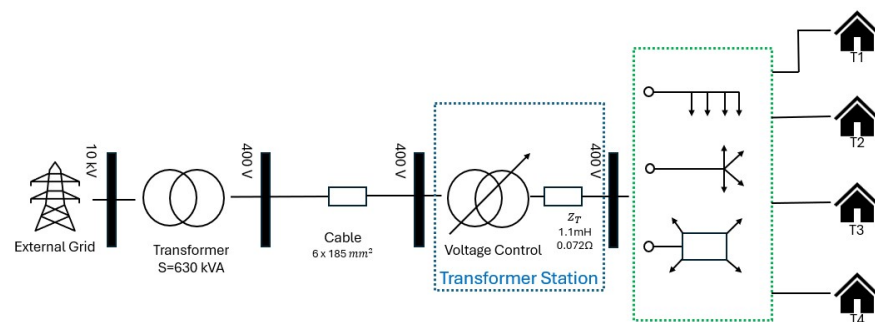


Figure 5. Smart grid lab in Austria with recreated distribution grid.

The Houses present in the UASTW laboratory’s electricity network are prosumers, i.e., they act simultaneously as consumers and producers of energy. Each house was connected to a smart meter, a photovoltaic system, a PV string simulator, controllable loads, and a battery storage system, and all the Houses are connected to the Austrian electricity grid. In addition, House T1 had the special feature of being connected to a charging station for electric vehicles, allowing this type of energy consumption to be integrated into the grid. Table 1 shows some of the main characteristics of the inverters analyzed here.

Table 1. Main technical characteristics of the inverters analyzed.

Equipment	MPP Voltage Range	Max. Output Power	Max. Output Current	Grid Connection
Fronius IG Plus (House T3)	230–500 V	2600 VA	11.3 A	1-NPE 230 V
Fronius Symo GEN24 (House T4)	278–800 V	10,000 VA	16.4 A	3-NPE 230 V
ENPHASE IQ7+ (Microinverter)	27–45 V	290 VA	1.26 A	1-NPE 230 V

### Experimental Setup

The UASTW laboratory has been able to simulate various controlled scenarios, with a particular focus on common everyday situations. Examples include the interaction of emissions from a PV inverter with emissions from an electric vehicle. It was also possible to connect different types of loads and analyze how they affect the electric grid, whether through SH emissions or by changing the impedance of the grid at higher frequencies. Figure 6 shows the types of loads that can be found in the UASTW laboratory.

### 3.2. Measurement Equipment

The measurement equipment used is the DEWE 800-PA power quality analyzer for capturing raw data. The DEWE-800-PA has a 16-bit resolution and offers a sampling rate of

1 MS/s per channel, with a basic accuracy of 0.02% for each of its 8 channels. For current measurement, a *Rogowski coil* was employed, offering a high bandwidth of 1 MHz and an accuracy of 1%. For voltage measurement, the *HSI-LV* module was used and connected via banana plugs, providing a bandwidth of up to 2 MHz.

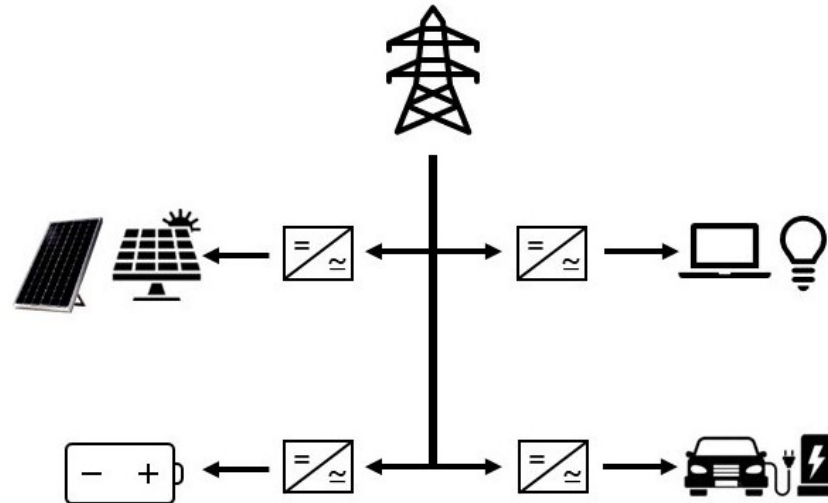


**Figure 6.** Possible equipment present in the laboratory. For example, these include PV systems, batteries, non-linear loads, and electric vehicle charging systems.

#### 4. Results and Discussion

This section presents the laboratory results related to SH emissions from PV inverters in an electrical distribution network. Different study scenarios were outlined using a microinverter and an inverter, with measurements conducted at the *UASTW* laboratory, which simulated a physical electricity distribution network.

##### 4.1. Evaluation of SH Emissions from the Inverter at House T3

The single-phase photovoltaic inverter Fronius IG Plus will be analyzed in this section. This device provides effective protection for both the operator and the equipment thanks to its galvanic isolation, which is equipped with an HF transformer. All measurements were conducted assuming a radial network topology.

###### 4.1.1. Case I

Figure 7 shows the frequency spectrum from 2 kHz to 150 kHz. Initially, a measurement of the inherent SH emissions from the electrical grid was carried out, and the inverter was not on in this scenario. It was observed that there were no emissions with significant amplitude. It is important to note the presence of SH emissions originating from the measuring equipment. Background emissions are shown in these images.

###### 4.1.2. Case II

This simulation was designed in an attempt to understand how different output power levels,  $P_{out}$ , of the inverter affect its SH emissions. Initially, through a careful analysis of the PV panel's IV curve and the MPPT point, it was determined that the inverter's output would present a current of 7A.

It is noteworthy that, in terms of the emission spectrum of current and voltage, there was a constant narrowband emission at a frequency of 20 kHz, seen in Figure 8, which served as a good indicator of the inverter's switching frequency and its corresponding emissions. It is also important to note that throughout the frequency range from 2 kHz to 9 kHz, there were constant SH emissions. According to the literature, harmonic emissions persist up to 9 kHz. In the current spectrum, a narrowband emission at 117 kHz was also observed, being likely attributable to emissions present in the electrical grid. Both the current and voltage spectra



indicate the presence of a narrowband emission around 10 kHz. It should be emphasized that current emissions are more detrimental than voltage emissions.

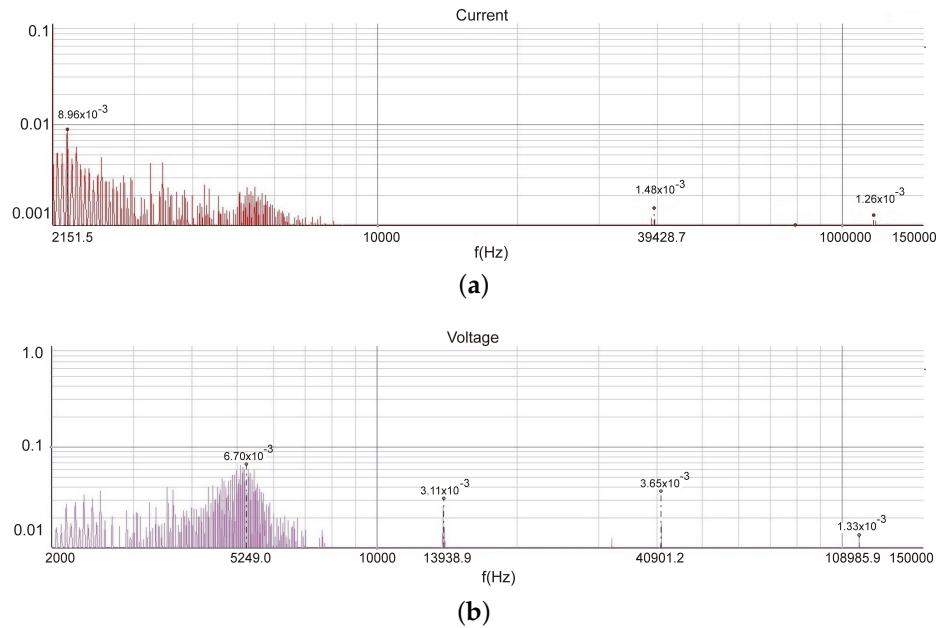


**Figure 7.** Analysis of the background emissions present in the grid: (a) current emission analysis; (b) voltage emission analysis.

Based on the analysis of Figures 8–10, which pertain to the scenario under study, it is important to highlight that, although SH emissions may appear constant to the naked eye when the inverter’s output current is reduced, this was not the case. The range of possible switching frequencies between the different  $P_{out}$  varied from 13 to 6 mA, which is a significant reduction. It should be noted that the cumulative impacts of SH emissions can destabilize the electricity grid if we consider much higher  $P_{out}$  values from different locations on the same electric grid.

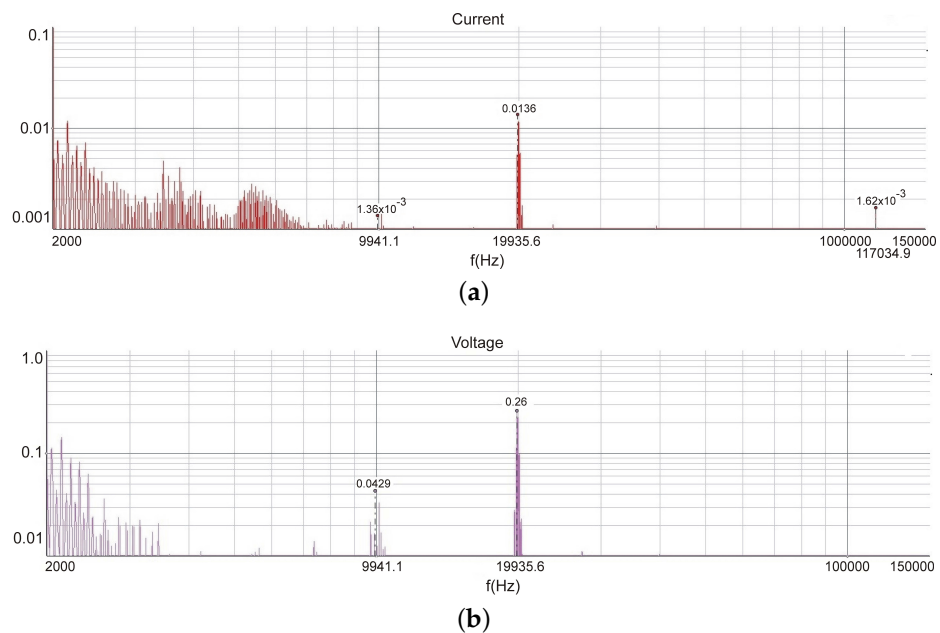


**Figure 8.** Analyses of SH emissions for a  $P_{out} = 7A$ : (a) current emission analysis; (b) voltage emission analysis.

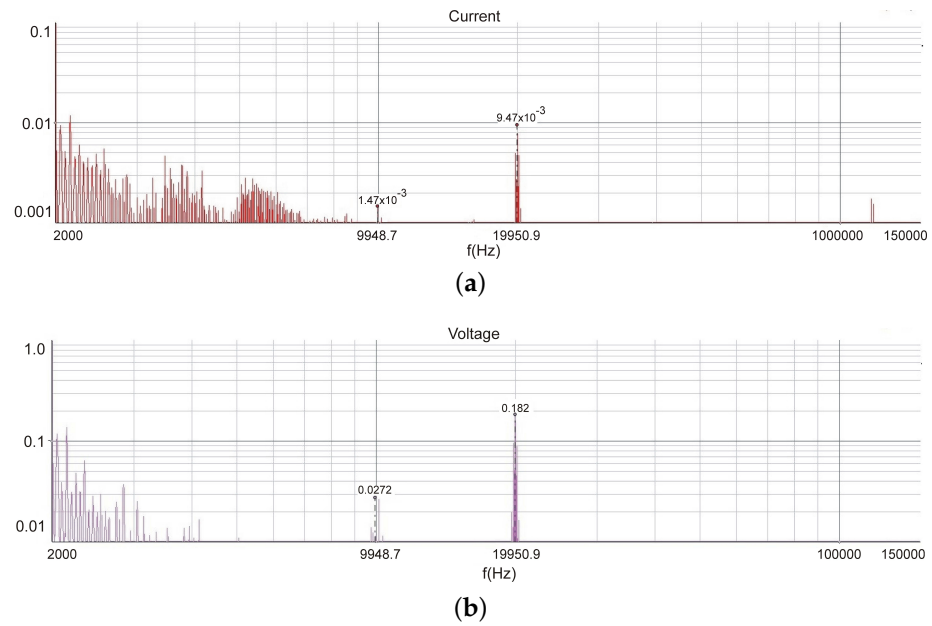


**Figure 9.** Analyses of SH emissions for a  $P_{out} = 5A$ : (a) current emission analysis; (b) voltage emission analysis.

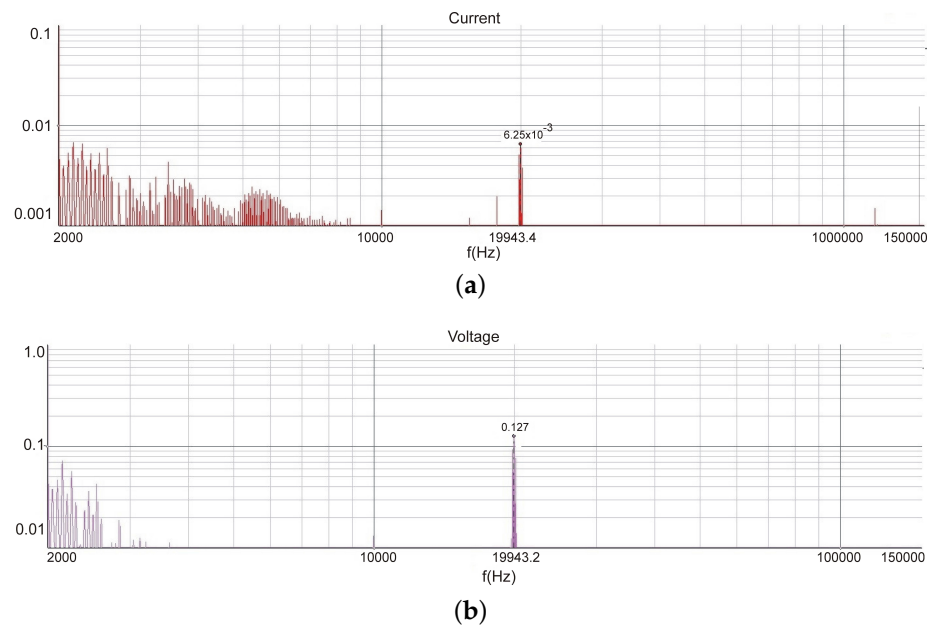


**Figure 10.** Analyses of SH emissions for a  $P_{out} = 1A$ : (a) current emission analysis; (b) voltage emission analysis.

#### 4.1.3. Case III

In this scenario, the interference of House T4 on the SH emissions of House T3 was analyzed. It is worth noting that House T4 has an inverter connected to the PV panels located on the *UASTW* balcony, meaning that the solar radiation on the day of measurement has a significant impact on its output power.

The need to distinguish between primary and secondary emissions becomes evident when observing Figures 11 and 12. The two measurements presented are from the same inverter, which were both taken at the inverter’s terminal under test, House T3, and the possible switching frequency (20 kHz) showed different amplitudes. It is noticeable that the amplitude was higher when House T4 was connected and operating, as shown in Figure 12. The inverter of House T4 was connected to the same phase as the inverter of House T3.

Two key observations become evident when analyzing the figures: the primary emission in the 20 kHz frequency range increased in amplitude as additional loads were connected, and the primary emissions from other devices propagated toward the inverter, contributing to secondary emissions at the terminal. When connected, House T4 was therefore responsible for the secondary emissions at the time of measurement. It displayed significantly lower power than the inverter of House T3, as the measurement was conducted in the morning when solar radiation was relatively low. The inverter’s switching frequency in the 20 kHz range was the dominant frequency component in both cases.

Furthermore, quantifying intermodulation in a real system presented significant challenges due to the complexity of identifying all the equipment influencing the network.

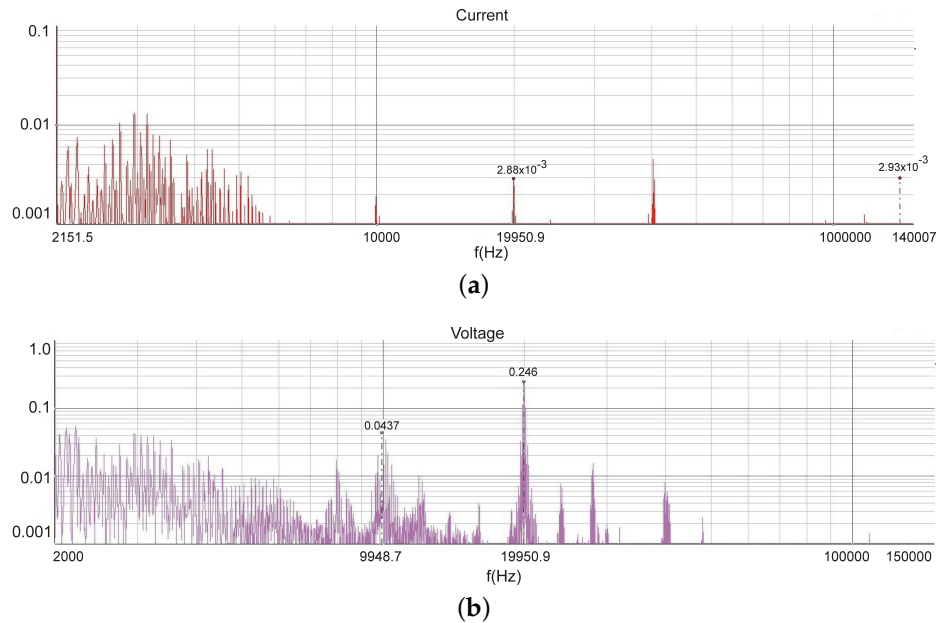


**Figure 11.** Analysis of SH emissions inverter during the initial stage of activation: (a) current emission analysis; (b) voltage emission analysis.

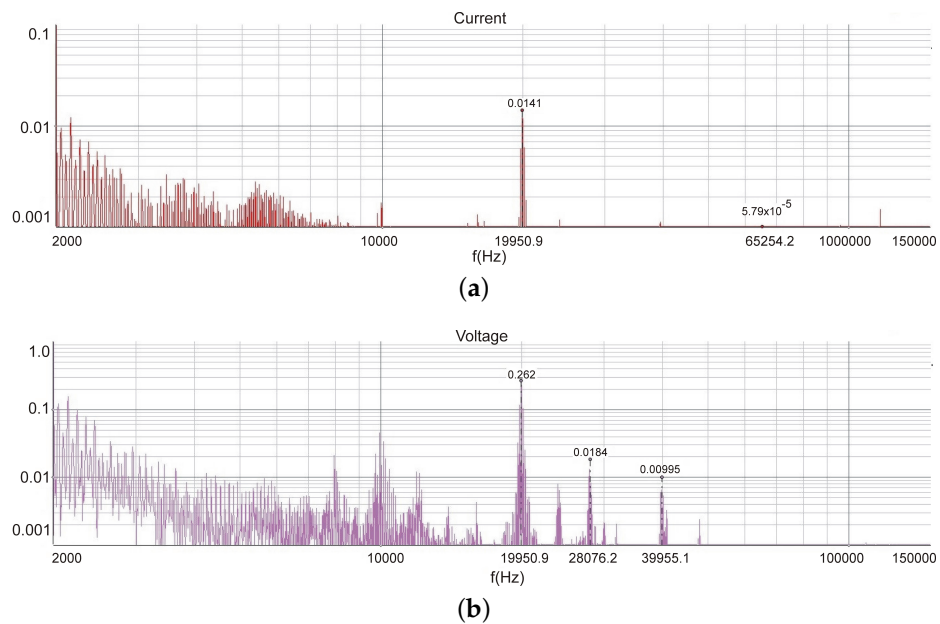


**Figure 12.** Analysis of SH emissions with inverter initialized: (a) current emission analysis; (b) voltage emission analysis.

#### 4.2. Evaluation of SH Emissions from the Microinverter

The single-phase ENPHASE IQ7+ microinverter has a nominal power of 290VA and uses PLC communication to connect to the optimizer, which serves to maximize energy production and improve system efficiency. The measurements were carried out using a luminaire specifically designed to simulate solar radiation.

In Figure 13, the first measurement, taken under low radiation conditions, is presented. Upon analysis, a possible switching frequency at 20 kHz can be observed. Figure 13 also shows the frequency spectrum of the emissions under medium and maximum radiation conditions, respectively. An initial analysis of the frequency spectra reveals that the emissions did not vary in amplitude depending on the radiation levels.

An analysis of Figure 14 allows for the identification of the frequency band in which PLC communication between the microinverter and the optimizer occurred within the current frequency spectrum. A peak emission at 120 kHz was noted. In summary, it was observed that, in all analyses, background emissions, secondary emissions, and primary emissions from the microinverter itself were prevalent. It is concluded, therefore, that the network under study was significantly impacted by SH emissions.

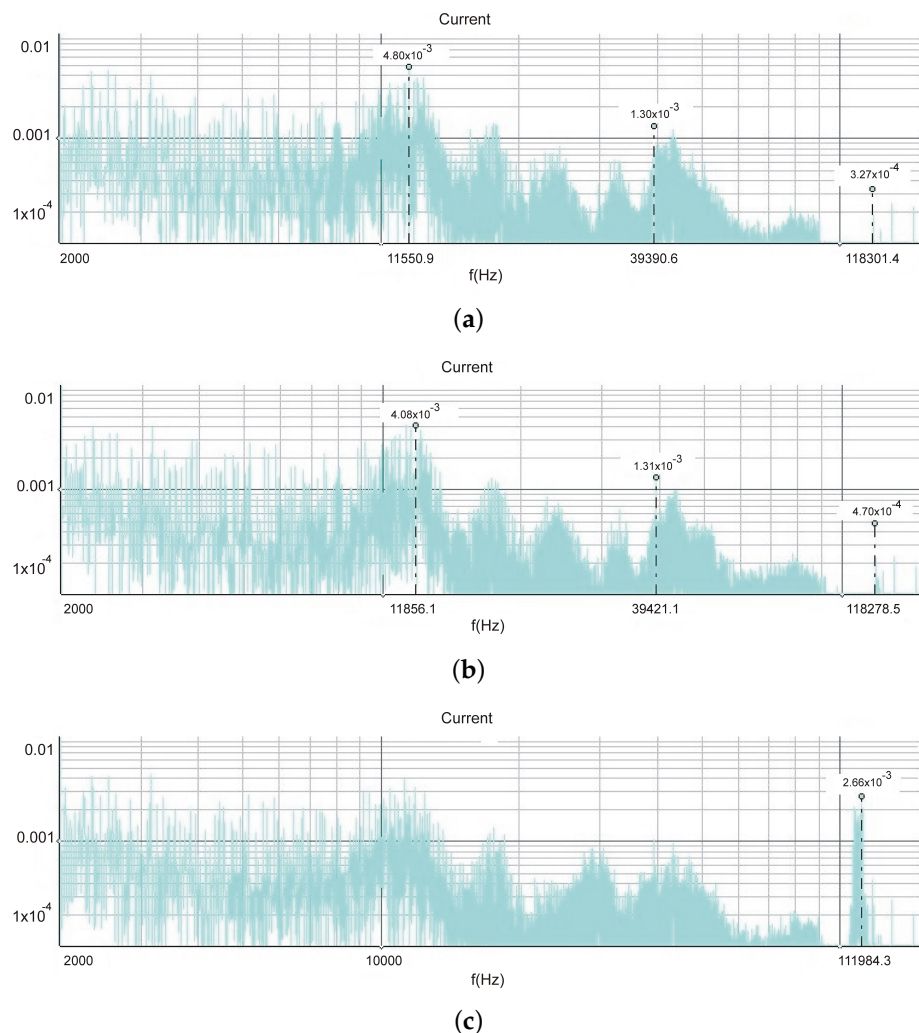


**Figure 13.** Analyzing current SH emissions: (a) low solar radiation; (b) mean solar radiation; (c) maximum solar radiation.

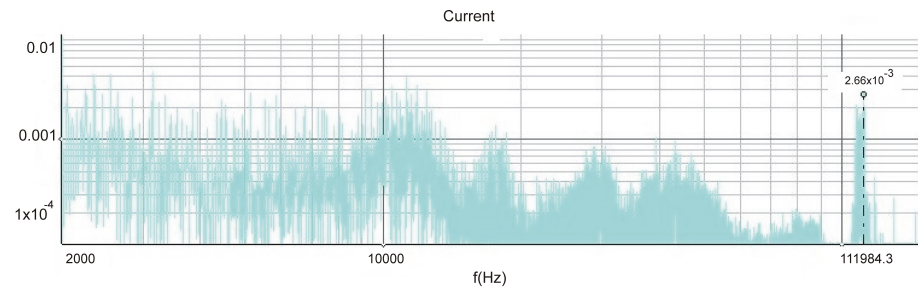


**Figure 14.** Spectral analysis of current emissions and corresponding PLC emissions.

#### 4.3. Results Discussion

It is well known that the current of an inverter typically has a phase shift close to  $90^\circ$  relative to the voltage due to the presence of a capacitor in the connection filter between the inverter and the grid. Most electronic devices contain capacitors specifically designed to eliminate HF noise from input signals. However, it is important to highlight that capacitors absorb HF components, as their impedance is inversely proportional to frequency, as indicated in Equation (6):

$$Z_C = \frac{1}{j2\pi fC} \quad (6)$$

where  $C$  represents capacitance, and  $f$  represents the frequency, which is expressed in Hz. This characteristic can result in significant heating, reducing the lifespan of these components and accelerating the degradation of the equipment itself. The integration between the grid and the filters influences the amount of current absorbed by other devices, altering the resonance frequencies.

When the inverter is connected in an environment with HF emissions, the capacitor provides a low impedance path, allowing HF components to propagate to the inverter while it is in operation. It is worth noting that even when the inverter is not in operation, it may generate HF emissions. The current measured at the terminal of an inverter connected to the electrical grid will consist of both primary and secondary emissions, which can result in the phenomenon known as intermodulation. In this way, a PV inverter influences HF emissions in both the grid and the installation through both the injection and absorption of these emissions.

Table 2 provides a comprehensive overview of the HF emissions recorded for the two PV inverters examined, which exhibited components at the threshold of the audible range for humans. The audible noise resulting from the interference of HF emissions can have a significant impact on various aspects of daily life.

The objective of these scenarios was to outline the behavior of HF emissions, identifying both primary and secondary emissions, as well as intentional and unintentional emissions. In one of the scenarios, the focus was on the interference of HF emissions from House T4 with those from House T3, with the aim of observing and understanding the intermodulation of HF emissions. An increase in the amplitude of primary emissions was observed with the connection of other loads. Another scenario analyzed the ENPHASE IQ7+ microinverter, where it was found that HF emissions remained constant regardless of variations in solar radiation.

It is important to highlight that these results underscore the relevance of the topology of electronic equipment in both the emission and mitigation of HF emissions. Depending on their topology, these devices can act as protective elements for the electrical grid by absorbing such emissions. Currently, this absorption occurs in a manner that is detrimental to the devices themselves due to their internal impedance. In the future, it is expected that these devices will be able to absorb emissions safely, benefiting both the equipment and the electrical grid to which they are connected.

The constant presence of HF emissions and the identification of specific PLC frequency bands reinforce the need for continuous monitoring and effective mitigation strategies to

maintain the integrity of the electrical grid and minimize the adverse impacts of these emissions. In summary, these results emphasize the importance of a comprehensive and detailed analysis of HF emissions, known as SHs, in different PV systems, contributing to the development of standards and regulations that ensure electromagnetic compatibility and energy efficiency in interconnected systems.

**Table 2.** Current SH emissions from the equipment analyzed. The values marked in red are within the human hearing range.

Equipment	Switching Frequency (kHz)	Amplitude (mA)
House T3	20	14.1
ENPHASE IQ7+	20	4.08

## 5. Conclusions

This paper addresses the issue of HF emissions, classified as SHs. SH emissions have been proliferating, particularly in low-voltage networks, due to the increasing use of technologies that produce distortions in the frequency range of 2 kHz to 150 kHz. Concerns related to power quality in electrical distribution networks have become significantly critical due to the rise in non-linear loads and the growing integration of renewable energy sources.

It is evident that intermodulation is independent of the energy production of PV systems. Once the equipment responsible for secondary emissions is disconnected, intermodulation distortion is no longer perceptible. Observations suggest that intermodulation between devices does not occur systematically, and the underlying mechanism of these interactions requires further investigation. From the perspective of the devices, intermodulation may result in immunity issues, highlighting the need for additional research.

The frequency at which SH emissions occur does not directly determine the frequencies of the oscillations observed later. While the amplitude of the emissions is a relevant factor, it is primarily the impedance and the topology of the equipment that dictate the conditions under which this phenomenon manifests itself.

SH emissions from grid-connected inverter systems have the potential to compromise the stability of the electrical infrastructure. Therefore, a precise understanding of the inherent impedance of the electrical grid is of utmost importance. In this context, the critical significance of estimating grid impedance must be highlighted. Regarding the grid's impedance, it is imperative to conduct a thorough analysis of its prediction and its impact on power quality, taking into account the possible effects of disturbances induced by grid-connected inverter systems—whether by creating low-impedance paths or attenuating emissions in cases of parallel resonances.

Emissions in the SH range predominantly flow between nearby devices, although some emissions also propagate through the electrical grid. The purpose of investigating the behavior of the electrical grid at higher frequencies is to understand how the connection of equipment utilizing active power electronics influences impedance. These findings are essential for clarifying the propagation of SH emissions in the 2 kHz to 150 kHz range.

In the context of SHs, two approaches remain to be considered for addressing the relevant issues: preventing the occurrence of these anomalies or mitigating them after they appear. Prevention requires an optimized decision regarding emissions vs. immunity, which must be deliberated by standardization committees in agreement with equipment manufacturers, whether or not their devices are responsible for SH emissions.

**Author Contributions:** Conceptualization, J.P., B.G., and J.B.; methodology, J.P., B.G., and J.B.; software, J.P., B.G., and J.B.; validation, J.P., B.G., and J.B.; formal analysis, J.P., B.G., and J.B.; investigation, J.P., B.G., and J.B.; resources, J.P., B.G., and J.B.; data curation, J.P., B.G., and J.B.; writing—original draft preparation, J.P., B.G., and J.B.; writing—review and editing, J.P., B.G., and

J.B.; visualization, J.P., B.G., and J.B.; supervision, J.P., B.G., and J.B.; project administration, B.G. and J.B.; All authors have read and agreed to the published version of the manuscript.

**Funding:** This research received no external funding.

**Data Availability Statement:** The data are contained within the article.

**Acknowledgments:** This research is supported by Vine and Wine Portugal—Driving Sustainable Growth Through Smart Innovation Mobilizing Agenda—whose project identifier is C644866286-011.

**Conflicts of Interest:** The authors declare no conflicts of interest.

## Abbreviations

The following abbreviations are used in this manuscript:

SHs	Supraharmonics
PV	Photovoltaic
HF	High-Frequency
EU	European Union
RNC	Roadmap for Carbon Neutrality
NDC	Nationally Determined Contribution
DC	Direct Current
AC	Alternating Current

## References

- Nations, U. Paris Agreement—Framework Convention on Climate Change. 2015. Available online: [https://unfccc.int/sites/default/files/english\\_paris\\_agreement.pdf](https://unfccc.int/sites/default/files/english_paris_agreement.pdf) (accessed on 18 January 2024).
- Republic, P. Roadmap to Carbon Neutrality. 2019. Available online: <https://www.portugal.gov.pt/download-ficheiros/ficheiro.aspx?=%3d%3dBAAAAB%2bLCAAAAAAABACzMDexAAAut9emBAAAAA%3d%3d> (accessed on 18 January 2024).
- Council of European Union. Directive (EU) 2019/944—Common Rules for the Internal Market for Electricity and Amending Directive 2012/27/EU. 2019. Available online: <https://eur-lex.europa.eu/legal-content/EN/TXT/PDF/?uri=CELEX:32019L0944> (accessed on 5 October 2024).
- Council of European Union. Directive (EU) 2018/2001—The Promotion of the Use of Energy From Renewable Sources. 2018. Available online: <http://data.europa.eu/eli/dir/2018/2001/oj> (accessed on 5 October 2024).
- Pradhan, S.; Singh, B.; Panigrahi, B.K. A Digital Disturbance Estimator (DDE) for Multiobjective Grid Connected Solar PV Based Distributed Generating System. *IEEE Trans. Ind. Appl.* **2018**, *54*, 5318–5330. [[CrossRef](#)]
- Pinto, R.; Calado, M.; Mariano, S.; Espírito-Santo, A. Micro-generation with solar energy: Power quality and impact on a rural low-voltage grid. In Proceedings of the 2015 9th International Conference on Compatibility and Power Electronics (CPE), Costa da Caparica, Portugal, 24–26 June 2015; pp. 87–92. [[CrossRef](#)]
- Li, C. Unstable Operation of Photovoltaic Inverter From Field Experiences. *IEEE Trans. Power Deliv.* **2018**, *33*, 1013–1015. [[CrossRef](#)]
- Slangen, T.; Čuk, V.; Cobben, J.; De Jong, E. Variations in Supraharmonic Emission (2–150 kHz) of an EV Fast Charging Station under Different Supply- and Operating Conditions. In Proceedings of the 2023 IEEE Power & Energy Society General Meeting (PESGM), Orlando, FL, USA, 16–20 July 2023; pp. 1–5. [[CrossRef](#)]
- Ceaki, O.; Vatu, R.; Mancasi, M.; Porumb, R.; Seritan, G. Analysis of electromagnetic disturbances for grid-connected PV plants. In Proceedings of the 2015 Modern Electric Power Systems (MEPS), Wroclaw, Poland, 6–9 July 2015; pp. 1–5. [[CrossRef](#)]
- Std 519-2014*; IEEE Recommended Practice and Requirements for Harmonic Control in Electric Power Systems; (Revision of IEEE Std 519-1992). IEEE: New York, NY, USA, 2014; pp. 1–29. [[CrossRef](#)]
- Std 1547-2003*; IEEE Standard for Interconnecting Distributed Resources with Electric Power Systems. IEEE: New York, NY, USA, 2003; pp. 1–28. [[CrossRef](#)]
- Grasel, B.; Baptista, J.; Tragner, M. The impact of V2G charging stations (active power electronics) to the higher frequency grid impedance. *Sustain. Energy Grids Netw.* **2024**, *38*, 101306. [[CrossRef](#)]
- He, L.; Xu, S.; Li, H.; Zhu, K.; Ji, Z. Analysis of the Supraharmonic Characteristics of VSR PWM Converter. In Proceedings of the 2023 IEEE 6th International Electrical and Energy Conference (CIEEC), Hefei, China, 12–14 May 2023; pp. 842–847. [[CrossRef](#)]
- Arrillaga, J.; Watson, N.R. *Power System Harmonics*, 2nd ed.; Wiley: Hoboken, NJ, USA, 2003.
- IEC 61000-4-7*; Electromagnetic Compatibility (EMC)—Part 4-7: General Guide on Harmonics and Interharmonics Measurements and Instrumentation, for Power Supply Systems and Equipment Connected Thereto. International Electrotechnical Commission: Geneva, Switzerland, 2002.
- IEC 61000-4-30*; Electromagnetic Compatibility (EMC)—Part 4-30: Power Quality Measurement Methods. International Electrotechnical Commission: Geneva, Switzerland, 2008.

17. CISPR 16; Specification for Radio Disturbance and Immunity Measuring Apparatus and Methods—Part 16. International Electrotechnical Commission: Geneva, Switzerland, 2010.
18. Grasel, B.; Reis, M.J.C.S.; Baptista, J.; Tragner, M. Comparison of Supraharmonic Emission Measurement Methods Using Real Signals of a V2G Charging Station and a PV Power Plant. In Proceedings of the 2022 International Conference on Smart Energy Systems and Technologies (SEST), Eindhoven, The Netherlands, 5–7 September 2022; pp. 1–6. [\[CrossRef\]](#)
19. Abid, F.; Busatto, T.; Rönnberg, S.K.; Bollen, M.H.J. Intermodulation due to interaction of photovoltaic inverter and electric vehicle at supraharmonic range. In Proceedings of the 2016 17th International Conference on Harmonics and Quality of Power (ICHQP), Belo Horizonte, Brazil, 16–19 October 2016; pp. 685–690. [\[CrossRef\]](#)
20. IEC 61000-2-2; Electromagnetic Compatibility (EMC)—Part 2-2: Environment—Compatibility Levels for Low-Frequency Conducted Disturbances and Signalling in Public Low-Voltage Power Supply Systems. International Electrotechnical Commission: Geneva, Switzerland, 2002.
21. Khokhlov, V.; Meyer, J.; Schegner, P. Thermal Interactions in Modern Lighting Equipment due to Disturbances in the Frequency Range 2–150 kHz. In Proceedings of the 2019 IEEE Milan PowerTech, Milan, Italy, 23–27 June 2019; pp. 1–6. [\[CrossRef\]](#)
22. Baptista, J.; Morais, R.; Valente, A.; Soares, S.; Candeias, M.; Reis, M. HarmoSim: A tool for harmonic distortion simulation and assessment of nonlinear loads. *Comput. Appl. Eng. Educ.* **2014**, *22*, 340–348. [\[CrossRef\]](#)
23. Grasel, B.; Baptista, J.; Tragner, M.; Leonhartsberger, K.; Keusch, G. Supraharmonic Emissions of a bidirectional electric vehicle charging station—A research methodology based on tests at reconstructed distribution grid. In Proceedings of the 2021 IEEE 4th International Conference on Power and Energy Applications (ICPEA), Busan, Republic of Korea, 9–11 October 2021; pp. 51–59. [\[CrossRef\]](#)
24. Slangen, T.; van Wijk, T.; Čuk, V.; Cobben, S. The Propagation and Interaction of Supraharmonics from Electric Vehicle Chargers in a Low-Voltage Grid. *Energies* **2020**, *13*, 3865. [\[CrossRef\]](#)
25. Mariscotti, A.; Mingotti, A. The Effects of Supraharmonic Distortion in MV and LV AC Grids. *Sensors* **2024**, *24*, 2465. [\[CrossRef\]](#) [\[PubMed\]](#)
26. Prudenzi, A.; Fioravanti, A.; Silvestri, A.; Ciancetta, F.; Fiorucci, E.; Mari, S. Overview of the Propagation of Supraharmonics in Power Systems. In Proceedings of the 2022 AEIT International Annual Conference (AEIT), Rome, Italy, 3–5 October 2022; pp. 1–6. [\[CrossRef\]](#)
27. Alfalahi, S.T.Y.; Alkahtani, A.A.; Al-Shetwi, A.Q.; Al-Ogaili, A.S.; Abbood, A.A.; Mansor, M.B.; Fazea, Y. Supraharmonics in Power Grid: Identification, Standards, and Measurement Techniques. *IEEE Access* **2021**, *9*, 103677–103690. [\[CrossRef\]](#)
28. Espín-Delgado, Á.; Rönnberg, S.; Sudha Letha, S.; Bollen, M. Diagnosis of supraharmonics-related problems based on the effects on electrical equipment. *Electr. Power Syst. Res.* **2021**, *195*, 107179. [\[CrossRef\]](#)

**Disclaimer/Publisher’s Note:** The statements, opinions and data contained in all publications are solely those of the individual author(s) and contributor(s) and not of MDPI and/or the editor(s). MDPI and/or the editor(s) disclaim responsibility for any injury to people or property resulting from any ideas, methods, instructions or products referred to in the content.